

Graphene in a photonic metamaterial

Nikitas Papasimakis,¹ Zhiqiang Luo,² Ze Xiang Shen,² Francesco De Angelis,^{3,4}
Enzo Di Fabrizio,^{3,4} Andrey E. Nikolaenko,¹ and Nikolay I. Zheludev^{1*}

¹Optoelectronics Research Centre, University of Southampton, Southampton SO17 1BJ, United Kingdom

²School of Physical and Mathematical Sciences, Nanyang Technological University, 637371 Singapore

³Italian Institute of Technology, 16163 Genova, Italy

⁴University of Magna Graecia, 88100 Catanzaro, Italy

*niz@orc.soton.ac.uk

Abstract: We demonstrate a photonic metamaterial that shows extraordinary sensitivity to the presence of a single atomic layer of graphene on its surface. Metamaterial's optical transmission increases multi-fold at the resonance frequency linked to the Fano-type plasmonic mode supported by the periodic metallic nanostructure. The experiments were performed with chemical vapor deposited (CVD) graphene covering a number of size-scaled metamaterial samples with plasmonic modes at different frequencies ranging from 167 to 187 THz.

©2010 Optical Society of America

OCIS codes: (160.3918) Metamaterials.

References and links

1. K. S. Novoselov, A. K. Geim, S. V. Morozov, D. Jiang, Y. Zhang, S. V. Dubonos, I. V. Grigorieva, and A. A. Firsov, "Electric field effect in atomically thin carbon films," *Science* **306**(5696), 666–669 (2004).
2. A. H. Castro Neto, F. Guinea, and N. M. R. Peres, "Drawing conclusions from graphene," *Physics World* **19**, 33–37 (2006).
3. K. S. Novoselov, E. McCann, S. V. Morozov, V. I. Fal'ko, M. I. Katsnelson, U. Zeitler, D. Jiang, F. Schedin, and A. K. Geim, "Unconventional quantum Hall effect and Berry's phase of 2π in bilayer graphene," *Nat. Phys.* **2**(3), 177–180 (2006).
4. Y. Zhang, Y. W. Tan, H. L. Stormer, and P. Kim, "Experimental observation of the quantum Hall effect and Berry's phase in graphene," *Nature* **438**(7065), 201–204 (2005).
5. X. Du, I. Skachko, A. Barker, and E. Y. Andrei, "Approaching ballistic transport in suspended graphene," *Nat. Nanotechnol.* **3**(8), 491–495 (2008).
6. A. K. Geim, and K. S. Novoselov, "The rise of graphene," *Nat. Mater.* **6**(3), 183–191 (2007).
7. M. Freitag, "Graphene: nanoelectronics goes flat out," *Nat. Nanotechnol.* **3**(8), 455–457 (2008).
8. M. Jablan, H. Buljan, and M. Soljacic, "Plasmonics in graphene at infrared frequencies," *Phys. Rev. B* **80**(24), 245435 (2009).
9. Z. H. Ni, H. M. Wang, J. Kasim, H. M. Fan, T. Yu, Y. H. Wu, Y. P. Feng, and Z. X. Shen, "Graphene thickness determination using reflection and contrast spectroscopy," *Nano Lett.* **7**(9), 2758–2763 (2007).
10. D. S. L. Abergel, A. Russell, and V. I. Fal'ko, "Visibility of graphene flakes on a dielectric substrate," *Appl. Phys. Lett.* **91**(6), 063125 (2007).
11. G. Teo, H. Wang, Y. Wu, Z. Guo, J. Zhang, Z. Ni, and Z. Shen, "Visibility study of graphene multilayer structures," *J. Appl. Phys.* **103**(12), 124302 (2008).
12. P. Blake, E. W. Hill, A. H. C. Neto, K. S. Novoselov, D. Jiang, R. Yang, T. J. Booth, and A. K. Geim, "Making graphene visible," *Appl. Phys. Lett.* **91**(6), 063124 (2007).
13. X. Wang, M. Zhao, and D. D. Nolte, "Optical contrast and clarity of graphene on an arbitrary substrate," *Appl. Phys. Lett.* **95**(8), 081102 (2009).
14. K. Chang, J. T. Liu, J. B. Xia, and N. Dai, "Enhanced visibility of graphene: Effect of one-dimensional photonic crystal," *Appl. Phys. Lett.* **91**(18), 181906 (2007).
15. A. Banerjee, and H. Grebel, "Depositing graphene films on solid and perforated substrates," *Nanotechnology* **19**(36), 365303 (2008).
16. V. A. Fedotov, M. Rose, S. L. Prosvirnin, N. Papasimakis, and N. I. Zheludev, "Sharp trapped-mode resonances in planar metamaterials with a broken structural symmetry," *Phys. Rev. Lett.* **99**(14), 147401 (2007).
17. A. Ishimaru, S. Jaruwatanadilok, and Y. Kuga, "Generalized surface Plasmon resonance sensors using metamaterials and negative index materials," *PIERS* **51**, 139–152 (2005).
18. I. A. I. Al-Naib, C. Jensen, and M. Koch, "Thin-film sensing with planar asymmetric metamaterial resonators," *Appl. Phys. Lett.* **93**(8), 083507 (2008).
19. T. Driscoll, G. O. Andreev, D. N. Basov, S. Palit, S. Y. Cho, N. M. Jokerst, and D. R. Smith, "Tuned permeability in terahertz split-ring resonators for devices and sensors," *Appl. Phys. Lett.* **91**(6), 062511 (2007).
20. C. Debus, and P. H. Bolivar, "Frequency selective surfaces for high sensitivity terahertz sensing," *Appl. Phys. Lett.* **91**(18), 184102 (2007).

21. B. Lahiri, A. Z. Khokhar, R. M. De La Rue, S. G. McMeekin, and N. P. Johnson, "Asymmetric split ring resonators for optical sensing of organic materials," *Opt. Express* **17**(2), 1107–1115 (2009).
22. H. J. Lee, and J. G. Yook, "Biosensing using split-ring resonators at microwave regime," *Appl. Phys. Lett.* **92**(25), 254103 (2008).
23. E. Cubukcu, S. Zhang, Y. S. Park, G. Bartal, and X. Zhang, "Split ring resonator sensors for infrared detection of single molecular monolayers," *Appl. Phys. Lett.* **95**(4), 043113 (2009).
24. X. S. Li, W. W. Cai, J. H. An, S. Kim, J. Nah, D. X. Yang, R. D. Piner, A. Velamakanni, I. Jung, E. Tutuc, S. K. Banerjee, L. Colombo, and R. S. Ruoff, "Large-area synthesis of high-quality and uniform graphene films on copper foils," *Science* **324**(5932), 1312–1314 (2009).
25. V. V. Khardikov, E. O. Iarko, and S. L. Prosvirnin, "Trapping of light by metal arrays," submitted for publication.
26. N. Papisimakis, V. A. Fedotov, Y. H. Fu, D. P. Tsai, and N. I. Zheludev, "Coherent and incoherent metamaterials and order-disorder transitions," *Phys. Rev. B* **80**(4), 041102 (2009).
27. V. A. Fedotov, N. Papisimakis, E. Plum, A. Bitzer, M. Walther, P. Kuo, D. P. Tsai, and N. I. Zheludev, "Spectral collapse in ensembles of meta-molecules," <http://arxiv.org/abs/0908.2533>.

1. Introduction

Graphene is a flat monolayer of carbon atoms arranged in a two-dimensional honeycomb lattice. Although theoretically studied for more than half a century it was believed unstable and only recently was its existence verified [1]. Owing to the 2D nature of the lattice, electrons in graphene have unique properties appealing to fundamental and applied physics alike. In particular, electrons in graphene behave as massless Dirac fermions providing an accessible system, where predictions of quantum electrodynamics can be tested [2,3]. Also, graphene demonstrates a particularly strong field-effect related to its ballistic electronic transport [1,4,5], that, combined with its planar nature, attracts a growing interest as a very promising candidate for nanoscale electronics [6,7]. On the other hand, however, the extraordinary electronic properties of graphene do not lead to equally exciting optical properties. Although graphene is known to support plasmons at THz frequencies [8], at optical wavelengths it is barely visible and special techniques are considered in order to verify its presence. Typically this means measuring reflection contrast of graphene deposited on a substrate using the substrate reflectivity as reference [9–12]. In this way, a maximum contrast of 15% can be achieved [13], which can be improved by the use of perforated substrates [14,15].

Here we study the electromagnetic response of a composite medium consisting of single-layer graphene deposited on a metamaterial that supports "trapped mode" plasmonic resonances. It consists of a two-dimensional array of asymmetrically-split ring slits on a gold film. Metamaterials of this type are known to show Fano anti-symmetric resonant lines in transmission with enhanced local fields that appear "trapped" in the vicinity of the nanostructure [16]. Such a configuration is of substantial interest both in terms of enabling high-contrast detection of graphene monolayers as well as in terms of possible metamaterial-based sensing applications, where graphene serves as a continuous adsorption layer. Indeed, in view of quantifying the sensitivity of possible metamaterial sensors [17], it has been observed that dielectric superstrates, such as photo-resists, deposited mainly on split-ring metamaterials result in strong frequency shifts of the metamaterial resonances throughout the electromagnetic spectrum, from microwave frequencies [18] to the sub-mm [19,20] and the infrared [21] range. In addition, it has been shown that the resonant split-ring properties can lead to the reliable detection of biomolecules [22] and single molecular monolayers [23]. In this letter, we show that graphene modifies dramatically the transmission spectrum of such a metamaterial leading to an increase of transmission exceeding 250%. This effect does not originate from the absorption of graphene but results from the renormalization of the plasmonic modes and the frequency shift of the trapped-mode transmission resonance in the presence of the highly polarizable graphene.

2. Samples and fabrication

The unit cell of the metamaterial contains an asymmetrically-split ring consisting of two slits in a gold film (see Fig. 1a). Metamaterials of this type support trapped modes, i.e. anti-symmetric field configurations which minimize radiation losses. Excitation of such a mode

leads to a dip in transmission (see Fig. 3a). The metamaterial structures were fabricated by focused ion beam milling through a 65 nm thick gold film evaporated on a 102 nm thick Si_3N_4 membrane. Gold film roughness of less than 5 nm was obtained with low pressure (10^{-8} mbar) thermal evaporation. We manufactured three almost identical sets of samples with five metamaterial arrays each. The overall size of the arrays was $22 \times 22 \mu\text{m}^2$, while the unit cell D varied among the five arrays from 711 nm to 839 nm. For wavelengths longer than the unit cell side, the metamaterial arrays do not diffract.

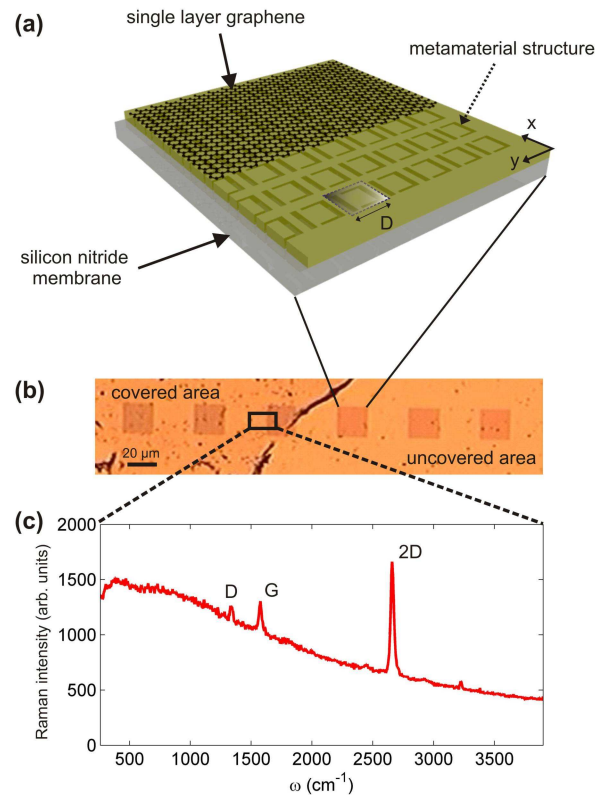


Fig. 1. (a) Schematic of the fabricated complementary split-ring metamaterial. (b) Microscope photograph of six metamaterial arrays after deposition of graphene: Note the boundary between the covered and non-covered areas. (c) Raman spectrum corresponding to the marked region in (b).

The graphene films were grown on polycrystalline Cu foils (99.95%, 34 μm thick, commercially available by Goodfellow) at temperatures up to 1000°C by low pressure CVD process [24] using a mixture of ethylene and hydrogen. After the growth, the graphene-on-Cu samples were coated with poly-methyl methacrylate (PMMA) and the PMMA/graphene films were separated from the Cu foils by etching in an aqueous solution of iron nitrate (0.2 M). The PMMA/graphene films were then transferred on to the substrates with the metamaterial structures, and the PMMA was removed by acetone. The graphene/metamaterial samples were rinsed several times by de-ionized water. Contrast and Raman spectroscopy and Raman mapping were carried out to assess the quality and uniformity of the CVD graphene with a WITTEC CRM200 Raman system using a 100X objective lens with a numerical aperture (NA) of 0.95. The excitation source for Raman spectroscopy was a 532 nm laser (2.33 eV) with a laser power at sample below 1 mW to avoid laser-induced heating.

Figure 1c shows a Raman spectrum with peaks typical for single layer graphene, including a 2D band with a full width at half-maximum (FWHM) of 30 cm^{-1} located at 2670 cm^{-1} and a

G band with a much lower Raman intensity than that of the 2D band. The weak D band peak at 1330 cm^{-1} activated by defects via a double resonance Raman process indicates that the graphene is of high quality with very few defects. The broad background originates from the Au film.

3. Experimental results

The spectral response of the metamaterial before and after graphene deposition was measured experimentally in a micro-photospectrometer (CRAIG). The electric field of the incident field was polarized along the y-axis of Fig. 1a. We quantified the induced change in the metamaterial transmission spectrum due to the presence of the graphene layer by $C = (T_g - T_0)/T_0$, where T_0 and T_g refer to the transmission of the metamaterial before and after the deposition of the graphene layer, respectively (see Fig. 2).

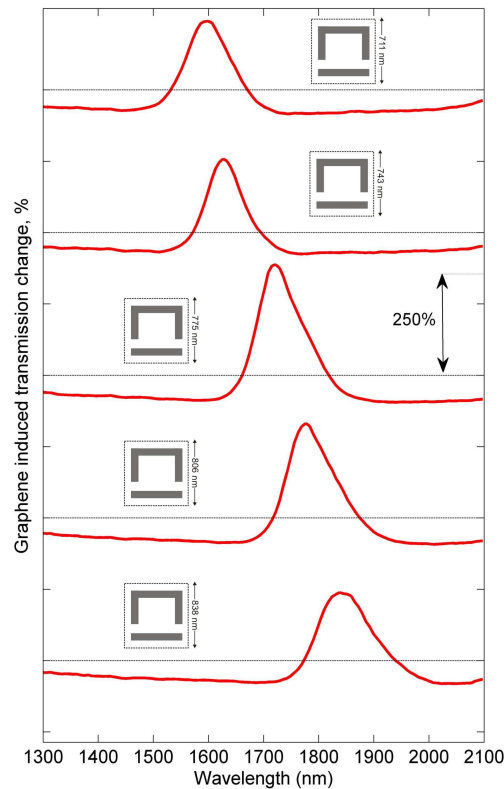


Fig. 2. Transmission contrast of the graphene covered metamaterial arrays for five different values of the unit cell side D , displaced along the vertical axis. Dashed black lines mark the zero contrast level.

In our experiment, part of the sample containing three metamaterial arrays of different unit cell sizes was not covered by graphene (see Fig. 1b), while the rest of the sample containing twelve different metamaterial arrays of five different sizes was covered by epitaxial graphene. Within experimental accuracy (which is essentially limited by the spectrometer's detector noise and by repositioning errors during repeated measurements), the transmission spectra of the uncovered samples before and after deposition of graphene remained unchanged indicating negligible contamination during the graphene transfer process. The transmission spectra of all the other metamaterial arrays have been modified dramatically by the graphene layer. The modification of the transmission spectra of different arrays with the same unit cell size was essentially the same: an intense peak of increased transmission exceeding 250%

appeared at the trapped-mode resonance frequency. Arrays of different unit cell size supporting trapped-mode resonances at different frequencies displayed the transmission increase at these frequencies: with increasing unit cell size, the peak in the contrast spectrum migrates towards longer wavelengths; a clear manifestation of their relation to the geometry of the metamaterial arrays. In Fig. 2, for presentation purposes the spectra corresponding to different unit cell sizes have been displaced along the vertical axis to avoid overlap.

4. Discussion

The origin of the peaks in the contrast spectrum can be understood by examining the metamaterial transmission spectrum before and after graphene deposition (see Fig. 3a). The transmission spectrum of the bare metamaterial shows a distinct peak, followed by a transmission dip (marked α) that we attribute to the trapped-mode resonance, while a second transmission peak (marked as β) can be seen at longer wavelengths. The effects of graphene as a metamaterial superstrate are consistent with that of a thin lossy dielectric superstrate characterized by permittivity ϵ with a non-zero imaginary part. The trapped-mode resonance shifts towards lower frequencies due to the polarizability of graphene, while due to Joule losses the resonance becomes broader with lower (higher) transmission at the transmission maxima (minimum). As a result, although transmission at the peak decreases, when transmission is monitored at a fixed wavelength, a strong increase will be observed due to the resonance shift.

This is further illustrated in Fig. 3b, where the relative resonance shift is presented as a function of the unit cell side. Here the relative shift is defined as $(\lambda_r - \lambda_i) / \lambda_i$, where λ_i and λ_r are the positions of the resonances (transmission dip (α) and the transmission peak (β)) before and after graphene deposition, respectively. A consistent wavelength shift varying between 5% and 10% is observed for all cases. Intriguingly, the long-wavelength transmission peak (β) appears to experience a much smaller wavelength shift than the trapped-mode resonance. Indeed, for all samples covered with the graphene layer, the wavelength shift is smaller than 2%, although transmission at the maximum drops significantly.

We attribute this difference in behavior to the peculiarities of the field structure associated with the trapped-mode and the long-wavelength resonance. This is illustrated in Fig. 3c by numerical simulations. At the trapped-mode resonance both slits are strongly excited, while at the long-wavelength resonance only the short slit is excited. In fact, the trapped-mode excitation of the unit cell includes a strong component of an electric dipole excitation perpendicular to the plane of the asymmetrically split ring (ASR). In contrast, within the unit cell, the excitation at the long-wavelength resonance is a magnetic dipole parallel to the array's plane (as it follows from Babinet's principle the excitations here are complementary to that of an asymmetric split-ring wire array [16,25]). We argue that this distinct difference in the nature of the two resonances coupled to the highly anisotropic electric and magnetic optical frequency polarizabilities of graphene leads to the different reactions of the metamaterial to the presence of the graphene layer: a strong response at the trapped-mode resonance frequency and a much weaker response at the long-wavelength resonance. Another hypothesis is that this difference may be emphasized by the collective nature of the trapped mode formed through interactions between a large number of meta-molecules [26,27]. These interactions are mediated by plasmon-polaritons on the unstructured part of the gold film which are strongly affected and damped by the presence of the graphene layer. In contrast, the magnetic dipole resonances depend on individual localized plasmons in the grooves that are not much affected by the presence of graphene.

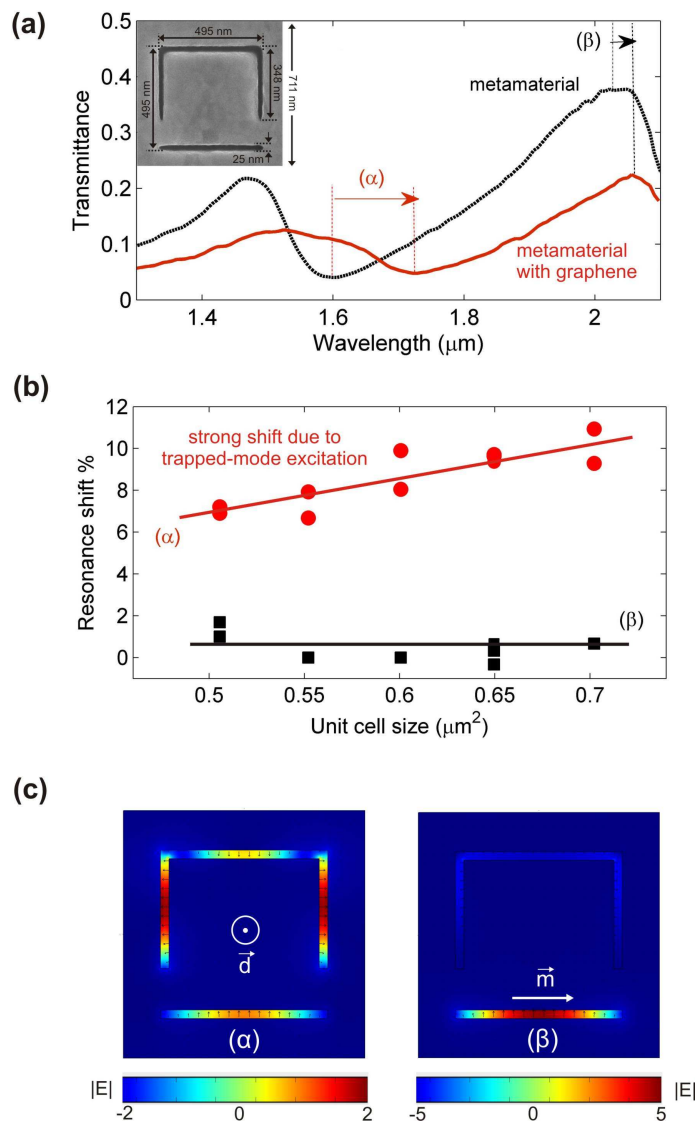


Fig. 3. (a) Experimental transmission spectrum of an ASR array before (dashed black line) and after (red solid line) deposition of graphene for unit cell size $D = 71$ nm as shown in the inset. The vertical dashed lines mark the position of the trapped-mode (α) and the long-wavelength dipole (β) resonance, before and after graphene deposition. (b) Wavelength shift of the trapped-mode (α) and of the dipole (β) resonance resulting from the deposition of the graphene layer as a function of unit cell size. (c) Electric field maps at the trapped-mode (α) and the dipole (β) resonance.

5. Conclusions

The sensitivity of the metamaterial to the presence of a single atomic layer of graphene on its surface is extraordinary. Indeed, more than 250% change in the transmission is caused by the graphene layer indicating that the structure can be used as an optical sensor detecting small concentrations of molecules adsorbed on the graphene membrane. In particular, the metamaterial can provide the narrow resonances needed for enhanced sensitivity, while the graphene layer allows the adsorption of molecules in the vicinity of the metamaterial surface. In fact, the presence of the graphene layer is essential as it allows to place the adsorbent at the

slits where the field is significantly enhanced. Then, we expect that the adsorbed molecules will modify the polarizability of the graphene monolayer, affecting thus the shape and position of the metamaterial resonances. We argue that adsorption of much less than a single atomic layer can be detected by monitoring transmission. Due to the strong field concentration in the slits only molecules adsorbed at the slit area matter. However, the area of the slits is less than 10% of the total surface of the metamaterial unit cell. Assuming a $100 \mu\text{m}^2$ area at the micro-spectrometer focal spot, we can expect that the adsorbent needs only to cover an area smaller than $10 \mu\text{m}^2$. On the other hand, by appropriate geometrical design, the Fano resonance can be shifted to any given frequency in the visible and the infrared parts of the spectrum to match the resonances of the adsorbed molecule thus increasing sensitivity even further. We plan to exploit the potential of metamaterials with graphene as a superstrate in sensing applications and test these expectations in the near future. We also intend to extend our studies to include multilayer graphene superstrates. Finally we plan to explore the effects, if any, of the periodic perturbation to the graphene layer due to the periodic patterning of the metamaterial and the oscillation potential that it presents at resonance.

In summary, we have demonstrated that trapped-mode metamaterial arrays constitute ideal substrates to enhance the transmission visibility of graphene in the optical part of the spectrum. The observed experimental ratios can exceed 250% with an absolute transmission level of about 10% at a specific wavelength that can be tuned in a broad spectral range by appropriate scaling of the metamaterial structure. This provides a very robust and simple method of detecting graphene and suggests optical sensor applications based on graphene-metamaterial systems.

Acknowledgement

The authors would like to acknowledge the financial support of the Engineering and Physical Sciences Research Council (U.K.) and the Royal Society.